ACADEMIC PRESS

Available online at www.sciencedirect.com
SCIENCE DIRECT®

Journal of Catalysis 216 (2003) 362–376

JOURNAL OF CATALYSIS

www.elsevier.com/locate/jcat

Hydrogenation/dehydrogenation reactions: isopropanol dehydrogenation over copper catalysts

R.M. Rioux and M.A. Vannice *

Department of Chemical Engineering, Pennsylvania State University, University Park, PA 16802, USA

Received 19 July 2002; revised 12 September 2002; accepted 9 October 2002

Abstract

For accurate catalyst comparisons and kinetic modeling, data free of mass and heat transfer effects must be acquired over a range of temperature and reactant concentrations using well-characterized heterogeneous catalysts. For semibatch reactors operated at constant pressure, selectivity vs conversion profiles at several temperatures, preferably obtained with catalysts reduced in situ, are required to allow complicated reaction networks to be defined. Vapor-phase isopropyl alcohol (IPA) dehydrogenation over carbon-supported Cu catalysts in a differential fixed-bed reactor was studied and compared to UHP Cu powder and a Cu chromite catalyst. Low dispersions of Cu (ca. 0.02–0.17) were obtained in all these catalysts. Cu dispersed on an activated carbon heat-treated at 1223 K had the highest turnover frequency (0.052 s^{-1} at 448 K) of all the Cu/C catalysts, more than double that on an industrial Cu chromite catalyst; thus the rate with this 5.0% Cu/C catalyst (6.0 μmol s^{-1} g^{-1}) was close to that of the chromite catalyst containing 41% Cu (10.6 μmol s^{-1} g^{-1}). The steady-state selectivity to acetone was 100% for all catalysts except those containing the nitric-acid-treated carbon. In the absence of Cu, the nitric-acid-treated carbon produced propylene under steady-state reaction conditions, and reduction at 573 K decreased activity compared to reduction at 423 K. This dehydration reaction is associated with the presence of oxygen-containing acidic groups on the C surface. The apparent activation energy for acetone formation was typically near 20 kcal mol^{-1} for all the Cu/C catalysts and the Cu powder, but it was near 12 kcal mol^{-1} for the Cu chromite catalyst. A DRIFT spectrum under reaction conditions indicated the presence of an isopropoxide species and molecularly adsorbed IPA on the surface. A Langmuir–Hinshelwood mechanism, which assumed removal of the first hydrogen atom as the rate-determining step and incorporated adsorbed IPA, hydrogen, acetone, and a surface isopropoxide species into the site balance, fit the kinetic data well and gave physically meaningful values for the enthalpies and entropies of adsorption.

Keywords: Isopropanol dehydrogenation kinetics; Copper catalysts; Carbon supports

1. Introduction

Catalytic hydrogenation and dehydrogenation reactions are commonly used in the chemical industry, and such reactions involving oxygenated compounds are particularly important in the preparation of pharmaceuticals and fine chemicals [1–4]. Many of these reactions are conducted in the liquid phase, with or without a solvent, typically under constant H_2 pressure, and such liquid-phase reactions involving oxygenates have recently been reviewed [3]. Older studies have historically reported results in the form of a product distribution (or selectivity) obtained after a given conversion (i.e., reaction time) in a batch or semibatch reactor at a given temperature with a certain weight of catalyst. Analytical difficulties certainly were a prime factor in establishing this format; regardless, little or no fundamental information was acquired about reaction pathways or specific activities. Lack of catalyst characterization to determine metal surface areas, as well as the infrequent use of in situ catalyst pretreatments, also contributed to the absence of information about specific activities, especially in obtaining a turnover frequency, i.e., TOF = molecule/s/Me_s, where Me_s is a surface metal atom. These same limitations existed with vapor-phase studies of hydrogenation/dehydrogenation reactions of organics [4]. Another limitation in many of these previous studies, particularly those involving liquid-phase reactions, was the non-use of any criterion, such as the Weisz parameter [5], the Thiele modulus [6], or the Madon–Boudart technique [7], to verify the absence of mass (and heat) transfer limitations.

Consequently, to acquire the information needed for accurate catalyst comparisons and kinetic modeling of these

* Corresponding author.
E-mail address: mavche@engr.psu.edu (M.A. Vannice).

0021-9517/03/$ – see front matter
doi:10.1016/S0021-9517(02)00035-0

reactions, modern studies must utilize well-characterized catalysts whose metal crystallite sizes and Me_s concentrations are known. Prereduced catalysts (preferably in situ) should be used, product selectivity as a function of conversion (and reaction time) in a semibatch reactor should be established because this is now easily done with current analytical techniques, and this last procedure should be done at different temperatures [3]. As a prelude to these kinetic studies, experiments must be conducted to verify the absence of mass (and heat) transfer effects. With such data, individual reactions can be modeled via a series of elementary steps utilizing either the steady-state approximation, a Langmuir–Hinshelwood model, or the microkinetic approach, and more complicated reaction networks can be described [3]. With such results, TOFs can be calculated and compared and the significance of parameters such as crystallite size, multimetallic composition, and metal–support interactions can be determined, although additional characterization may be required at times. Although they have shown promise [3], these latter concepts have not yet been applied to most of the important reactions representing the chemical industry; hence future studies offer the possibility of improving rates and selectivities via heterogeneous catalysts.

Although studied and utilized to a much lesser extent than hydrogenation reactions, dehydrogenation reactions involving organic compounds can also play an important role in the production of fine chemicals. Dehydrogenation reactions are typically endothermic and conversions can be equilibrium-controlled; in addition, low H_2 pressures may enhance deactivation due to coking, and a selectivity consideration of dehydrogenation versus dehydration as well as hydrogenolysis can become important when oxygenates are the reactants. Earlier kinetic studies of such reactions are not numerous [4]; hence, thorough kinetic studies of such reactions are needed to compare new types of catalysts and to formulate reaction models. Such an approach is reported here.

In addition, researchers are challenged today to develop processes that have minimal detrimental effects on the environment, and applications of "environmental catalysis" are increasing in such diverse areas as alternative fuels and global pollution clean-up and control [8,9]. Processes are needed in which the production of extraneous waste or byproducts is minimized and spent catalysts can be regenerated or utilized elsewhere after their lifetimes as catalysts have expired. The dehydrogenation of alcohols to aldehydes or ketones is a well-known industrial process, and these reactions are primarily carried out on copper catalysts because of their high selectivity to the dehydrogenation product [2]. The principal catalyst that has been used in these reactions is copper chromite; however, new EPA restrictions now prohibit the disposal of chromite in landfills. Thus, there is an incentive to develop new replacement Cu catalysts which contain no chromium. In this study copper was dispersed on an activated carbon which had been given different pretreatments, and the isopropanol dehydrogenation reaction was chosen to probe catalytic behavior and allow comparisons among these Cu/C systems, Cu chromite, and Cu powder. The kinetics of isopropanol dehydrogenation were determined and a reaction model was proposed which provides a rate expression consistent with these results along with meaningful thermodynamic parameters. Characterization of these catalysts by counting the concentration of surface Cu atoms allowed specific activities in the form of turnover frequencies to be calculated.

2. Experimental

2.1. Carbon supports

The as-received activated carbon (SX-1, Norit Corp.) used in this study has a specific surface area of 800 $m^2\,g^{-1}$ and a pore volume of 0.5 $cm^3\,g^{-1}$, and this original sample is designated AC-ASIS. A portion of this AC-ASIS carbon was soaked for 12 h in 12 N nitric acid (J.T. Baker) at 363 K to place oxygen-containing groups on the surface. After 12 h in HNO_3, the carbon was filtered from the nitric acid, washed with copious amounts of distilled, deionized (DD) water, dried overnight at 393 K, and stored in a desiccator until further use. This carbon is designated AC-HNO_3. A high-temperature-treated (HTT) carbon sample was produced by placing a portion of the AC-ASIS carbon in ceramic boats and heating to 1223 K in flowing H_2, holding at 1223 K for 6 h, cooling to room temperature under H_2, and exposing briefly to air. This sample, designated AC-HTT-H_2, was then stored in a desiccator. Graphite fibers, designated GF, were Thornel P25 pitch-based commercial fibers (Amoco Performance Prod.) which were first cut and then ground with a mortar and pestle into a fine powder which had a BET area of 6 $m^2\,g^{-1}$ [10].

2.2. Catalyst preparation

All activated carbon-supported Cu catalysts were prepared by a wet impregnation technique in which 0.5 cm^3 of an aqueous solution of $Cu(NO_3)_2 \cdot xH_2O$ (Aldrich, 99.999%) in DD water was added per g carbon [11]. After impregnation, these catalysts were dried overnight at 393 K and stored in a desiccator. Cu was deposited on the GF support by an ion exchange technique [12–15] employing an aqueous solution of $Cu(NO_3)_2 \cdot xH_2O$ and a concentrated NH_4OH solution. The $Cu(NO_3)_2$ solution was added dropwise over a period of 30 min while a pH of 10 was maintained for the duration of the stirring. Prior to any further characterization, catalyst samples were pretreated in situ at 1 atm in 50 sccm He for 1 h at either 423, 473, or 573 K, followed by reduction in 50 sccm H_2 at the same temperature for 4 h. Actual Cu loadings were determined by inductively coupled plasma emission-mass spectrometry at the Materials Characterization Laboratory at Penn State University.

A Cu chromite catalyst (Cu1800P, Engelhard Corp.) was used as received, and its specifications indicated 41 wt%

Cu and a surface area of 28 $m^2\,g^{-1}$ [16]. Ultrahigh-purity (UHP) Cu powder (Alfa Aesar, 99.999%) was cleaned by heating at 573 K for 15 min in a mixture of 10% O_2 in He before the normal catalyst pretreatment procedure was used.

2.3. Catalyst characterization

These Cu catalysts were characterized by selective CO, H_2, and oxygen chemisorption (via N_2O decomposition), and by X-ray diffraction (XRD) using procedures described elsewhere [17]. Briefly, H_2 and CO uptakes at 300 K were determined volumetrically in a stainless steel adsorption system providing a vacuum below 10^{-6} Torr in the sample cell and employing a digital pressure gauge (Mensor, Model 2101). The dual isotherm method, with an interim 1-h evacuation, was used to measure total and reversible H_2 and CO adsorption, and the irreversible CO adsorption was used to count Cu^{+1} sites [18]. The H_2 (MG Ind., 99.999%), CO (MG Ind., 99.99%), and N_2O (MG Ind., 99.99%) were flowed through separate molecular sieve traps (Supelco) and Oxytraps (Alltech Asso.) before use. Dissociative N_2O adsorption at 363 K was used to determine the metallic surface copper (Cu^0) site concentration, and these amounts were measured both volumetrically in the above system, using a liquid N_2 cold finger to freeze out residual N_2O [11], and gravimetrically in a thermal gravimetric analysis (TGA) system (P–E TGS-2). CO uptakes at 300 K were also determined in the TGA system for comparison [11]. Ar BET isotherms at 77 K were obtained in the volumetric system after heating the sample to 423 K under flowing He.

X-ray diffraction (XRD) spectra were obtained ex situ using a Rigaku Geigerflex diffractometer equipped with a Cu-K_α radiation source and a graphite monochromator. Each sample was given the desired pretreatment and then passivated by exposure to a flowing mixture of 1% O_2 in He at 300 for 1 h prior to handling in air during XRD measurements. Cu crystallite sizes were calculated from the linewidth at half height of the primary Cu^0 and Cu_2O peaks using the Scherrer equation with Warren's correction for instrumental line broadening.

2.4. Kinetic studies

Vapor-phase isopropyl alcohol (IPA) dehydrogenation was conducted in a differential microreactor to determine the kinetic behavior of this reaction. H_2 (MG Ind., 99.999%) and He (MG Ind., 99.999%) flowrates were regulated by needle valves and monitored by Hasting–Raydist mass flowmeters. Isopropyl alcohol (Acros Org., Fisher Sci., 99+%) was degassed either by three freeze/thaw cycles with liquid N_2 or by bubbling N_2 through it for 1 h. The IPA was pumped by a Sage Instruments syringe pump (Model 341A) into a heated stainless steel line where it was vaporized. During experiments to examine the effect of acetone (Aldrich Chem., 99.9+%) on reaction kinetics, a second syringe pump (KD Sci.) was used. All lines before and after the reactor were held at 393 K to avoid any condensation, and the effluent composition was analyzed with a Hewlett–Packard 5890 gas chromatograph equipped with a Porapak T column (Supelco) [11]. For a kinetic study, 20–100 mg of catalyst was loaded into the reactor and pretreated in situ for 4 h at either 473 or 573 K under 50 sccm H_2. At a selected set of conditions, the reaction was run for 60 min before a data point was taken. Standard conditions for IPA dehydrogenation activity at 1 atm were 14 Torr C_3H_7OH, no H_2 (balance He), and Arrhenius plots were obtained by varying the temperature in both ascending and descending order to verify reproducible activities. Partial pressure dependencies on IPA, H_2 and acetone were obtained at four different temperatures—433, 448, 458, and 473 K—for kinetic modeling purposes. During an IPA partial pressure study, the IPA pressure was varied from 7 to 50 Torr, while during a hydrogen study, the pressure of IPA was held at 14 Torr while the H_2 partial pressure was varied from 5 to 170 Torr, and during the acetone study, IPA and H_2 partial pressures were held at 14 and 0 Torr, respectively, as the acetone pressure was varied from 2 to 15 Torr. The uncertainties in the results were ±5% for reaction orders and ±3 kcal mol^{-1} for activation energies, while the reproducibility of TOF values was above 90%. Additional details are provided elsewhere [11]. Rates for the Cu/C catalysts, reported in μmol $g_{cat}^{-1}\,s^{-1}$, were corrected for any contribution from the carbon support when necessary, then normalized per mole of surface Cu^0 plus Cu^{+1} species ($Cu_s^0 + Cu_s^{+1}$) to obtain a turnover frequency, i.e., TOF = molecule $Cu_s^{-1}\,s^{-1}$.

2.5. DRIFTS (*diffuse reflectance infrared fourier transform spectroscopy*)

In order to enhance the low signal-to-noise ratio inherent with carbon samples, the Cu/C catalysts were diluted with calcium fluoride to give a CaF_2:Cu/C ratio of 30:1, and these diluted samples were loaded into the DRIFTS (HVC-DPR, Harrick Sci. Corp.) cell and purged with He overnight. Each sample was then given an in situ pretreatment and after cooling to the appropriate temperature the first interferogram was recorded using a Sirius 100 FTIR system (Mattson Inst. Inc.). This interferogram was used as the background reference for the fast Fourier transform analysis of all subsequent interferograms for that particular catalyst. The IPA partial pressure was obtained by flowing 20 sccm UHP He through an IPA saturator held at 279 K in a cyclohexane (99+%, A.C.S. reagent)/liquid N_2 slush bath [19], and spectra were recorded for each catalyst under the appropriate reaction conditions. The spectrum of vapor–phase IPA, which was used to subtract the vapor-phase contribution from the in situ reaction spectrum, was obtained by passing 14 Torr IPA in He over an Al mirror placed in the DRIFTS reactor cell. Details of the DRIFTS system and its modifications have been presented previously [20,21].

Table 1
Impurities in Norit SX—1 carbon (AC-ASIS)[a]

Element	Amount (wt%)
Al	0.07
Ba	< 0.02
Ca	0.05
Co	< 0.02
Cr	< 0.02
Cu	< 0.02
Fe	0.04
K	< 0.02
Mg	0.06
Mn	< 0.02
Na	0.12
Ni	< 0.02
P	< 0.02
S	0.13
Si	1.7
Ti	< 0.02
V	< 0.02
W	< 0.02
Zn	< 0.02
Zr	< 0.02

[a] By inductively coupled plasma analysis.

3. Results

3.1. Carbon supports

The three different Norit carbon samples were characterized by Ar BET and XRD, and their activity for vapor-phase isopropyl alcohol decomposition was studied to determine if the pure carbons had any intrinsic activity for either dehydrogenation or dehydration. A spectrochemical analysis of this Norit carbon provided the results in Table 1. Significant amounts of Si, Na, and S were present, and this level of sulfur, which can poison metal catalysts, is the reason to use the HTT, which removes sulfur from the carbon surface [22].

The total surface area (TSA) of each carbon after a given pretreatment, determined by Ar BET measurements at 77 K, is listed in Table 2. The surface area of AC-ASIS increased by 300 $m^2\,g^{-1}$ after high-temperature treatment (HTT), while it decreased by about 200 $m^2\,g^{-1}$ after a nitric acid treatment (HNO_3), which is attributed to the blockage of pores due to the creation of oxygen–containing functional groups. Additional characterization information has been provided previously [10].

Table 2
BET surface areas of pure carbons after reduction

Carbon	T_{RED} (K)	Surface area ($m^2\,g^{-1}$)
AC-ASIS	As-received	806
	423	814
	473	788
	573	769
AC-HNO_3	As prepared	616
AC-HTT-H_2	As prepared	1137
	473	1159
	573	1210

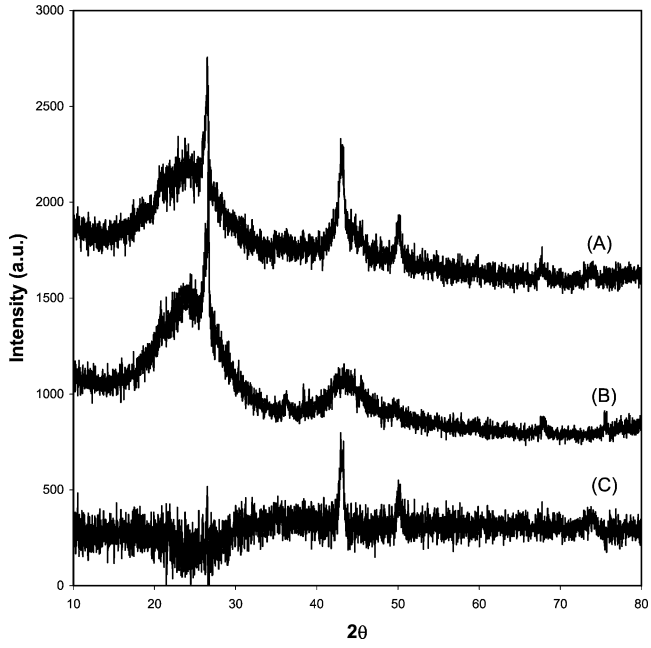

Fig. 1. X-ray diffraction patterns: (A) 5.01% Cu/AC-HTT-H_2 reduced at 573K; (B) AC-HTT-H_2 reduced at 573K; (C) after subtraction of (B) from (A).

Peaks observed in the XRD pattern at 2θ values of 24.1° and 25.2° for AC-ASIS and GF, respectively, are due to the (002) graphitic basal plane reflection, which reflects a decrease in the crystallinity that broadens the XRD peaks and shifts the (002) reflection towards lower angles [10]. A high degree of randomness in AC-ASIS and GF is further confirmed by a weaker, broad peak around 43°, indicative of the merging of the (100) and (101) plane into a single (10) plane. An example of this XRD pattern is given in Fig. 1 (Spectrum B), and it did not change significantly after pretreatment or reduction. Fig. 1 also provides a typical spectrum for a Cu/C catalyst showing the principal Cu^0 peaks at 43.29°, 50.34°, and 74.13°. The first peak was used to calculate crystallite size. In some samples, peaks were observed at 35.54°, 38.94°, and 36.42°which were due to CuO and Cu_2O, respectively.

Chemisorption on the pure carbons was measured using both volumetric and gravimetric techniques [11]. For all carbons, the irreversible CO uptake was close to zero. The amount of N_2O decomposed at 363 K on AC-ASIS to give surface oxygen was 4.9 $\mu mol\,O\,g^{-1}$, whereas it varied from 2.3 to 13.1 $\mu mol\,O\,g^{-1}$ for AC-HTT-H_2, depending on the pretreatment. No "O" adsorption on GF was measured at 363 K, and hydrogen adsorption was nil on all carbon samples. The results are summarized in Table 3.

3.2. Cu catalysts

The Cu catalysts and their Cu loadings are listed in Table 4. A representative pair of isotherms for CO uptakes

Table 3
H_2, CO, and oxygen adsorption on pure carbons

Catalyst	T_{RED} (K)	H_2 uptake[a] (μmol g^{-1})	CO uptake[b] (μmol g^{-1})		"O" uptake[c] (μmol g^{-1})
			Total	Irreversible	
AC-HNO_3	473	0.0	4.6	0.5	0.0
	573	0.0	11.8	0.5	0.0
AC-ASIS	423	–	48.5	0.2	0.0
	473	–	52.6	0.6	4.9
	573	–	49.1	0.0	4.9
AC-HTT-H_2	423	–	47.1	0.0	13.1
	473	0.0	55.4	0.0	2.3
	573	0.0	51.4	0.0	7.4
GE-IE[d]	473	–	2.0	0.0	0.0
	573	–	2.0	0.0	0.0

[a] Values extrapolated to zero pressure.
[b] Uptake at RT and 75 Torr CO.
[c] Irreversible "O" uptake via N_2O decomposition at 363 K and 75 Torr.
[d] From Ref. [4].

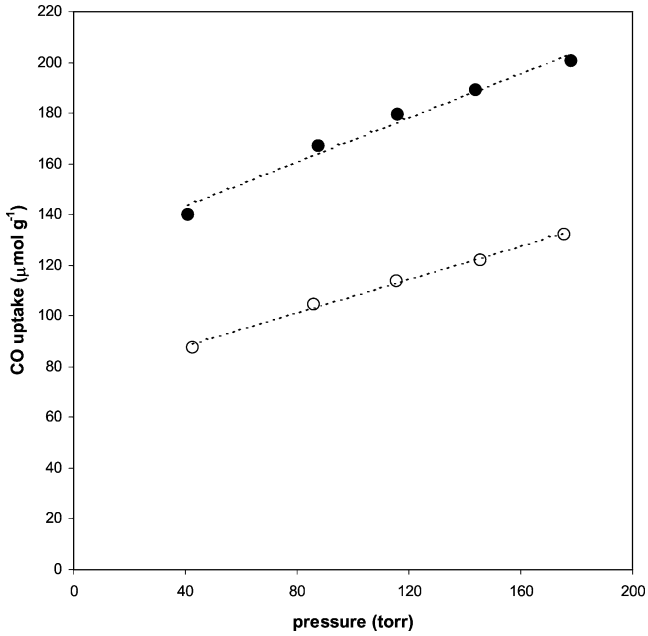

Fig. 2. CO chemisorption on 4.96% Cu/AC-HNO_3 reduced at 423K: total uptake (●), reversible uptake (○).

on 4.96% Cu/AC-HNO_3 reduced at 423 K is shown in Fig. 2, while other isotherms are provided elsewhere [11], and uptakes obtained from these isotherms are listed in Table 4. Irreversible CO uptakes on Cu catalysts are typically associated only with cuprous oxide, i.e., Cu_s^{+1} sites, whereas the total CO uptake minus that adsorbed on the support can provide an approximate measure of the total concentration of surface Cu atoms independent of the oxidation state [17,18]. Consequently, a dispersion ($D = Cu_s/Cu_T$, where Cu_s and Cu_T represent surface and total Cu atoms, respectively) can be estimated from the CO_T/Cu_T ratio.

The amount of metallic surface copper atoms can be measured by the dissociative chemisorption of N_2O after a prescribed pretreatment according to the following surface stoichiometry [18]:

$$2Cu_s + N_2O(g) \rightarrow Cu_s\text{–}O\text{–}Cu_s + N_2(g). \quad (1)$$

Fig. 3 represents a typical TGA experiment, and the adsorption of O atoms based on the final weight changes obtained in the TGA apparatus are also listed in Table 4. Based on these measurements, the "O" uptake on each Cu/C catalyst tended to increase as the reduction temperature in-

Table 4
CO and oxygen chemisorption on Cu catalysts

Catalyst	T_{RED}	CO uptake[a] (μmol g^{-1})		CO_T/Cu_T	CO_{irr}/Cu_T	"O" uptake[b]	Cu^0	d[c]
	(K)	Total	Irreversible			(μmol g^{-1})	Disp.	(nm)
4.96% Cu/AC-HNO_3	423	170.0	62.0	0.216218	0.078079	12.1	0.0.031032	35
	473	35.4	6.1	0.045	0.0078	18.3	0.0460.048	2423
	573	19.6	0.0	0.025	0.0	16.5	0.0420.043	26
4.89% Cu/AC-ASIS	423	54.0	0.0	0.068070	0.0	0.0	–	–
	473	54.6	0.0	0.069071	0.0	8.8	0.0220.023	5048
	573	51.6	0.0	0.066067	0.0	16.6	0.0420.044	2625
5.01% Cu/AC-HTT-H_2	423	79.4	5.7	0.101	0.0072	54.0	0.14	8.07.9
	473	83.5	5.6	0.106	0.0071	58.9	0.15	7.37.2
	573	59.1	0.0	0.075	0.0	67.3	0.17	6.46.3
0.98% Cu/AC-HTT-H_2	473	52.5	1.1	0.333340	0.007	11.1	0.1415	7.87.5
	573	53.2	0.0	0.0338345	0.0	8.9	0.1112	9.89.3
0.63% Cu/GF-IE	573	0.0	0.00	0.0	0.0	0.9[d]	0.019	58
Cu powder	573	–	–	–	–	1.8[d]	0.00023	4800
Cu chromite	573	55.0	18.3	0.0085	0.0028	181.5	0.056057	20

[a] Volumetric uptakes at 75 Torr corrected for irreversible uptake on support.
[b] Uptakes at 363 K and 75 Torr N_2O determined gravimetrically.
[c] Cu crystallite size based on $d = 1.1/(2\ O_{ad}/Cu_T)$.
[d] Determined volumetrically.

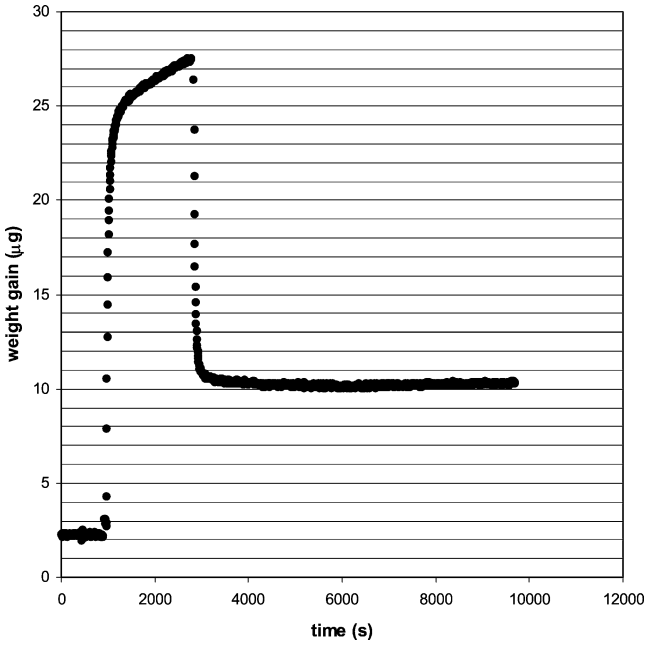

Fig. 3. Oxygen adsorption via N_2O decomposition at 363 K and 75 Torr N_2O on 5.01% Cu/AC-HTT-H_2 after reduction at 573 K.

creased. Metallic copper dispersions calculated from the O uptakes and the corresponding Cu^0 crystallite sizes, based on the relation $d(\text{nm}) = 1.1/D = 1.1/(2\ O_{ad}/Cu_T)$, are also reported in Table 4. High dispersions were not achieved with any catalyst, and the variation in dispersion obtained with the activated carbon catalysts is attributed to the different treatments given the carbon prior to impregnation. An alternate way to estimate the overall Cu dispersion after a given pretreatment is to add the number of Cu_s^0 atoms, represented by twice the O uptake, and the number of Cu_s^{+1} atoms, as measured by the irreversible CO uptake at 300 K. These values are also given in Table 5, along with the average crystallite sizes based on either XRD or chemisorption results using the relation $d(\text{nm}) = 1.15/[(Cu_s^0 + Cu_s^{+1})/Cu_T]$, which represents an average of the crystallite sizes for Cu^0 and Cu_2O, to estimate crystallite size in the latter case [17,18]. The pure carbon support XRD pattern was subtracted from that for the Cu/C catalyst before line widths and crystallite sizes were determined.

3.3. Kinetics of IPA decomposition

The decomposition of IPA, including both dehydration and dehydrogenation, was studied over these activated carbon samples. The relative initial activity for dehydration was AC-HNO_3 ≫ AC-ASIS > AC-HTT-H_2, but only AC-HNO_3 retained any steady-state activity. Both AC-ASIS and AC-HTT-H_2 produced propylene initially, but this activity decreased to zero after 1 and 6 h on stream, respectively. All catalysts also had an initial activity (after $\frac{1}{2}$ h on stream) for dehydrogenation, but this was rapidly lost. A significant decrease in the dehydration activity of AC-HNO_3 resulted by increasing the pretreatment temperature from 423 to 573 K, and these decreases in activity were attributed to the loss of acid sites. The results for the carbon samples are given in Table 6.

Steady-state activities and turnover frequencies for IPA dehydrogenation were measured over a temperature range of 423–473 K for a series of Cu catalysts after various pretreatments, and these values at 448 K are listed in

Table 5
Average Cu crystallite size (nm) from chemisorption and XRD techniques

Catalyst	T_{RED}	Based on XRD			Based on adsorption		Dispersion[d]
	(K)	CuO[a]	Cu_2O[b]	Cu[c]	Cu^0/Cu_T	$(Cu^{1+} + Cu^0)/Cu_T$	
4.96% Cu/AC-HNO_3	423	–	–	–	35	9.8	0.1103
	473	–	3.3	–	24	20	0.056
	573	–	–	10.2	26	25	0.043
4.89% Cu/AC-ASIS	423	–	–	10.7	–	0.0	–
	473	–	7.9	8.5	50	70	0.023
	573	–	–	8.5	26	25	0.044
5.01% Cu/AC-HTT-H_2	423	8.3	–	10.6	8.0	7.5	0.147
	473	–	–	14.9	7.3	6.9	0.160
	573	–	–	13.7	6.4	6.3	0.175
0.98% Cu/AC-HTT-H_2	473	–	–	13.9	7.8	7.1	0.14854
	573	–	–	11.3	9.8	9.3	0.118
0.63% Cu/GF-IE	423	–	–	10.3	–	–	–
	573	–	–	15.5	58	58	0.019
Cu chromite	573	–	–	17.0	20	18.2	0.060
Cu powder	573				4800	ND[e]	–

[a] Calculated from reflection at $2\theta = 38.94°$.
[b] Calculated from reflection at $2\theta = 36.42°$.
[c] Calculated from reflection at $2\theta = 43.29°$.
[d] Based on $(Cu^0 + Cu^{1+})/Cu_T$.
[e] Not determined.

Table 6
Isopropyl alcohol decomposition on pure activated carbons

Carbon	Red. temp	Activity[a] (μmol IPA $g^{-1}\,s^{-1}$)		Areal rate[a] (μmol $m^{-2}\,s^{-1} \times 10^4$)		E_a[b] (kcal mol^{-1})	Initial selectivity (%)	
	(K)	Initial	Steady state	Initial	Steady state		Propylene	Acetone
AC-HNO_3	423	0.52	0.09	8.4	1.4	20	0.9	0.1
	573	0.07	0.06	1.1	0.95	25	1.0	0.0
AC-ASIS	423	0.13	0.0	1.6	0.0	–	0.66	0.34
	573	0.02	0.0	0.0	0.0	–	1.0	0.0
AC-HTT-H_2	423	0.05	0.0	0.44	0.0	–	0.57	0.43
	573	0.0	0.0	0.0	0.0	–	–	–

[a] Initial rates measured at 423 K after $\frac{1}{2}$ h on stream, $P_{Ipa} = 14$ Torr.
[b] Activation energy for IPA dehydration.

Table 7. The TOFs were calculated based on the total number of Cu surface atoms ($Cu_s^0 + Cu_s^{+1}$) reported in Table 5. No activity was obtained with the Cu/graphitized fiber catalyst, and a wide range of activity existed among the other catalysts; for example, after reduction at 573 K, activity varied over 1000-fold and a similar, but smaller, variation existed in TOF values. Djéga-Mariadassou et al. have shown that IPA dehydrogenation over different crystal faces of ZnO is a structure-insensitive reaction [23], while Sinfelt et al. have found cyclohexane dehydrogenation to be structure-insensitive over Cu–Ni bimetallic catalysts [24]. Echevin and Teichner have shown convincingly that the dehydrogenation of butan-2-ol is structure-insensitive on Cu/Al_2O_3 catalysts; i.e., for 18 catalysts with a 10-fold variation in dispersion, a turnover frequency near $0.0027\,s^{-1}$ was measured at 451 K [25]. If the Cu/AC-ASIS catalyst is excluded because of possible contamination due to sulfur poisoning, the data in Table 7 show less than an order of magnitude variation in TOF over a relatively small variation in crystallite size (9–17 nm), and TOF values are quite similar for the Cu powder, the Cu chromite, and the two Cu/Ac-HTT-H_2 samples that have been cleaned of sulfur.

The selectivity to acetone is defined as (mol acetone)/(mol acetone + mol propylene), and the only catalyst that produced any propylene was the nitric-acid-treated carbon catalyst, regardless of reduction temperature. Dehydration to propylene is attributed to a reaction on the carbon surface catalyzed by acidic surface groups (carboxylic acids, lactones, quinones, etc.). The steady-state selectivity to propylene at 448 K over the acid-treated carbon decreased from 35 to 15% as the reduction temperature was increased from 423 to 573 K, and this decrease in selectivity is directly

Table 7
Isopropyl alcohol dehydrogenation over Cu catalysts (reaction conditions: $P_{Ipa} = 14$ Torr, $T = 448$ K)

Catalyst	T_{RED}	Cu species[a]	Dispersion[b]		Activity[c]	TOF[d]	E_a[e]	Selectivity (%)	
	(K)	initially	(Cu_s^0/Cu_T)	(Cu_s^{+1}/Cu_T)	(μmol $g^{-1}\,s^{-1}$)	($s^{-1} \times 100$)	(kcal mol^{-1})	Acetone	Propylene
4.96% Cu/AC-HNO_3	423	Cu^{+1}, Cu^0	0.031	0.078	0.57	0.53	19.4 (20.2)	65	35
	473	Cu^0	0.046	0.0078	0.13	0.36	19.2 (21.6)	56	44
	573	Cu^0	0.042	0.0	0.25	0.69	15.9 (17.1)	85	15
4.89% Cu/AC-ASIS	473	Cu^{+1}	0.022	0.0	0.03[f]	0.035[f]	28.4	100	0
	573	Cu^0	0.042	0.0	0.003[g]	0.0083[g]	25.7	100	0
5.01% Cu/AC-HTT-H_2	473[h]	Cu^{+1}	0.0	0.093	2.2	4.3	21.3	100	0
	473	Cu^{+1}, Cu^0	0.149	0.0	6.0	5.2	22.5	100	0
	573	Cu^0	0.171	0.0	2.7	2.0	21.4	100	0
0.98% Cu/AC-HTT-H_2	473	Cu^0	0.141	0.0	0.77	3.5	20.1	100	0
	573	Cu^0	0.112	0.0	0.38	2.2	20.5	100	0
0.63% Cu/GF-IE	573	–	0.0	0.019	nil	–	–	–	–
Cu powder	573	Cu^0	0.00023	0.0	0.2	6.2	20.6	100	0
Cu chromite	573	Cu^0	0.056	0.0028	10.6	2.8	11.7	100	0

[a] Predominant Cu surface species determined by CO chemisorption at 300 K and N_2O decomposition at 363 K.
[b] Dispersion based on $2(O_{ad})$ for Cu^0 and irreversible CO chemisorption for Cu^{+1} sites.
[c] Steady-state disappearance of IPA at 448 K and 14 Torr C_3H_7OH.
[d] Based on ($Cu_s^0 + Cu_s^{+1}$) surface sites.
[e] For acetone formation (values in parentheses for propylene formation).
[f] Values measured at 448 K after 24 h on stream.
[g] Extrapolated values. Reaction temperature was 493 K.
[h] Pretreated in He only.

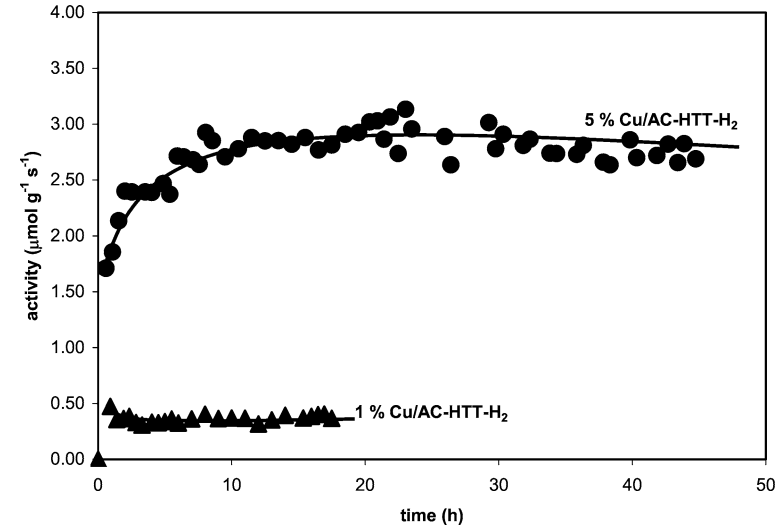

(A)

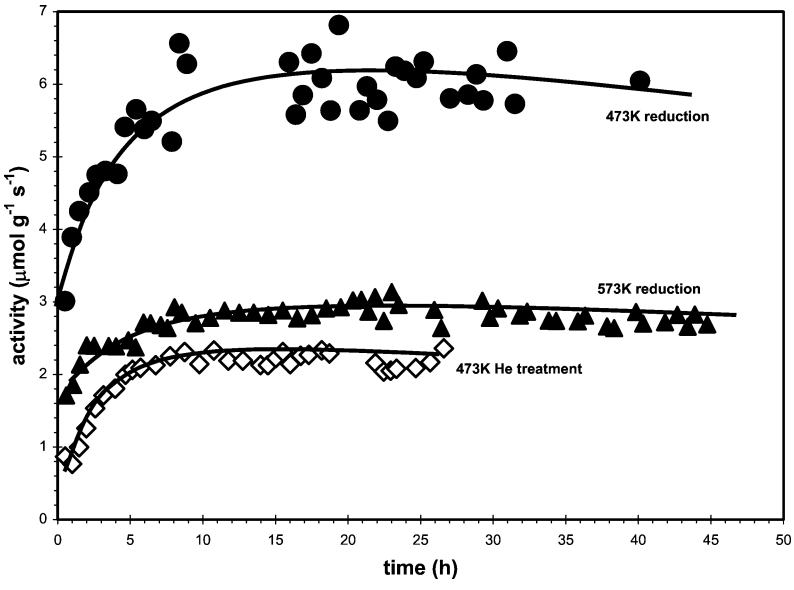

(B)

Fig. 4. (A) Isopropyl alcohol dehydrogenation activity profile for 0.98% and 5.01% Cu/AC-HTT-H_2 after reduction at 573 K. Reaction conditions: 25 ml min^{-1} total flow, 14 Torr IPA and 448 K. (B) Isopropyl alcohol dehydrogenation activity profile for 5.01% Cu/AC-HTT-H_2 subjected to different pretreatment conditions. Reaction conditions: 25 ml min^{-1} total flow, 14 Torr IPA, and 448 K.

related to the concentration of acidic sites on the carbon surface remaining after pretreatment.

Activity maintenance profiles for the 0.98% and 5.01% Cu/AC-HTT-H_2 catalysts are provided in Fig. 4A, and Fig. 4B shows the effect of pretreatment on 5.01% Cu/AC-HTT-H_2. After ∼7 hours on stream, the steady-state activity of the He-treated 5.01% Cu/AC-HTT-H_2 sample was comparable to that of the sample reduced at 573 K in H_2. The effect of the reduction temperature on the activity and selectivity of the 4.96% Cu/AC-HNO_3 catalyst is shown in Fig. 5. The absence of mass transfer effects was verified, as the Weisz criterion [5] routinely gave values far below 0.01 [11].

The Arrhenius behavior of each Cu catalyst was measured over an appropriate temperature range within which differential reaction conditions could be maintained, i.e.; the conversion never exceeded 15%, and the results are in Fig. 6. Apparent activation energies for dehydrogenation to acetone are listed in Table 7 and range from 11 to 28 kcal mol^{-1}, while the activation energy for propylene production was about 20 kcal mol^{-1}, which was quite similar to that with the carbon-only sample. The higher dehydrogenation activation energy with 4.89% Cu/AC-ASIS is attributed to impurities which most likely were removed during the nitric acid treatment (HNO_3) or the high-temperature treatment (HTT-H_2). This reaction is mildly endothermic ($\Delta H_R = +13.3$ kcal mol^{-1} at 298 K), and thermodynamic calculations showed that, under our typical reaction conditions, equilibrium conversions ranged from 34% at 423 K to 83% at 520 K [11]. In all cases, the activation energy for a given

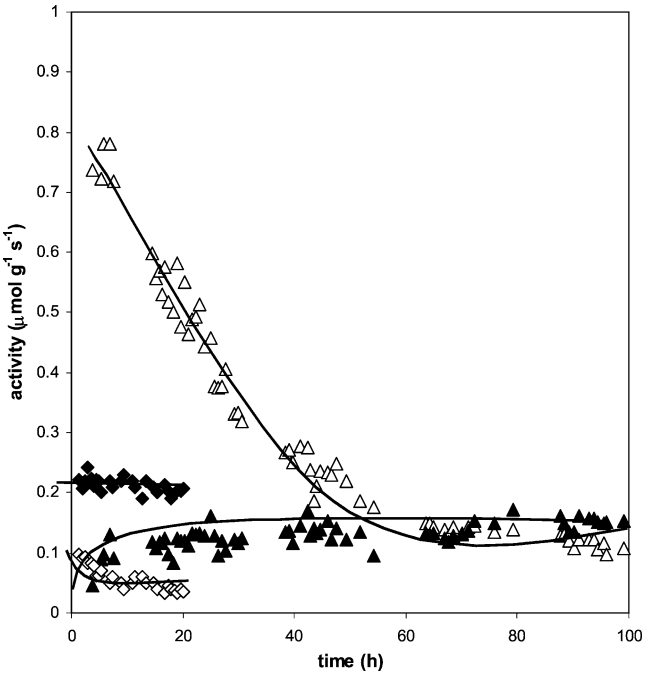

Fig. 5. Isopropyl alcohol activity profile for 4.96% Cu/AC-HNO_3 reduced at 423 K (▲) or 573 K (♦). Reaction conditions: 25 ml min^{-1} total flow, 14 Torr isopropanol, and 448 K. Acetone: solid symbols; propylene: open symbols.

catalyst did not vary significantly with pretreatment temperature.

For kinetic modeling purposes, partial pressure dependencies during IPA dehydrogenation were determined at 433, 448, 458, and 473 K with the 0.98% Cu/AC-HTT-H_2 catalyst after reduction at 573 K, and these results are shown

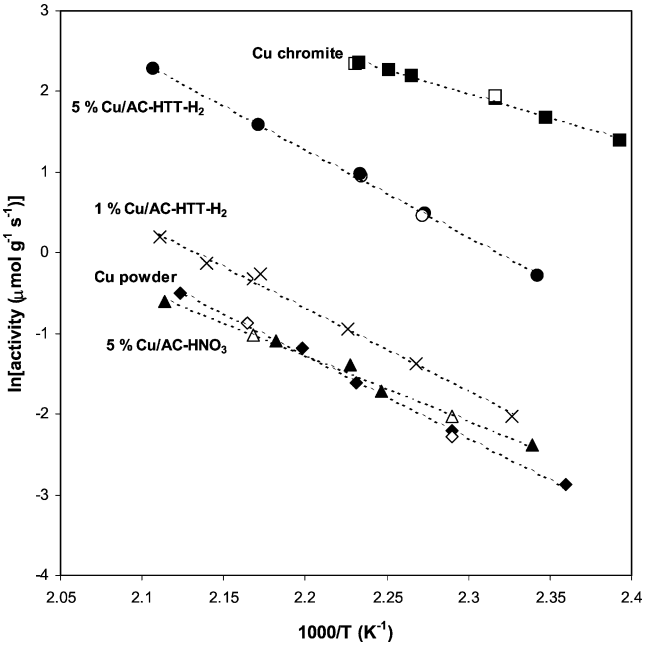

Fig. 6. Arrhenius plots for Cu catalysts reduced at 573 K. Reaction conditions: 14 Torr IPA and 448 K.

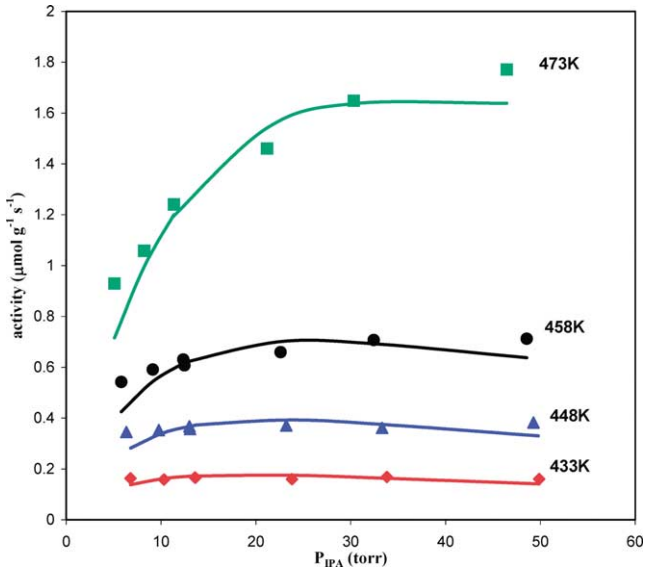

Fig. 7. Dependency of activity on IPA partial pressure for 0.98% Cu/AC-HTT-H_2 reduced at 573 K; symbols: experimental data, lines: rates predicted by Eq. (17) and Table 9.

in Figs. 7–9. Reaction orders for IPA, hydrogen, and acetone obtained from a power rate law using these data points are listed in Table 8 from graphs shown elsewhere [11]. The data indicate a dependence on IPA between zero and one-half while those on H_2 and acetone are zero or slightly negative.

A DRIFT spectrum with the 0.98% Cu/AC-HTT-H_2 catalyst under reaction conditions of 14 Torr IPA at 448 K is shown in Fig. 10. The vapor-phase spectrum of IPA has been subtracted; thus signature absorption bands from vapor-phase isopropyl alcohol are absent. A spectrum taken under identical conditions using only CaF_2 was completely fea-

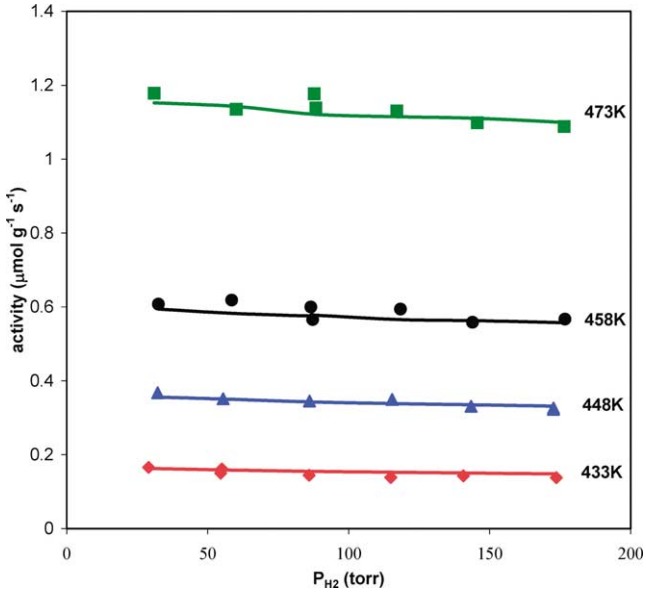

Fig. 8. Dependency of activity on H_2 partial pressure for 0.98% Cu/AC-HTT-H_2 reduced at 573 K; symbols: experimental data, lines: rates predicted by Eq. (17) and Table 9.

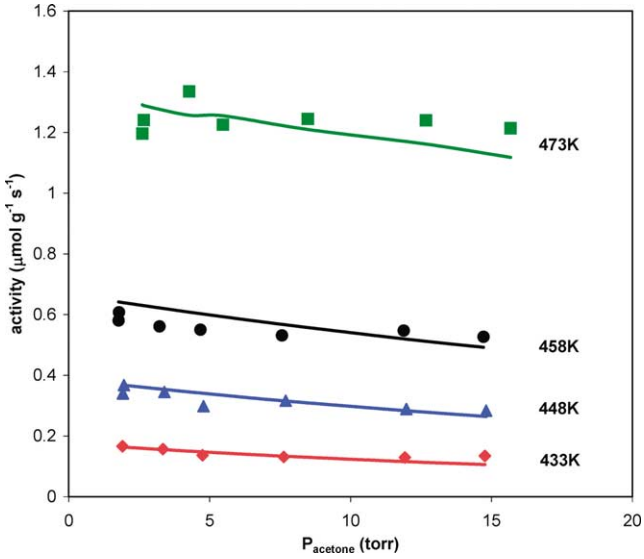

Fig. 9. Dependency of activity on acetone partial pressure for 0.98% Cu/AC-HTT-H_2 reduced at 573 K; symbols: experimental data; lines: rate predicted by Eq. (17) and Table 9.

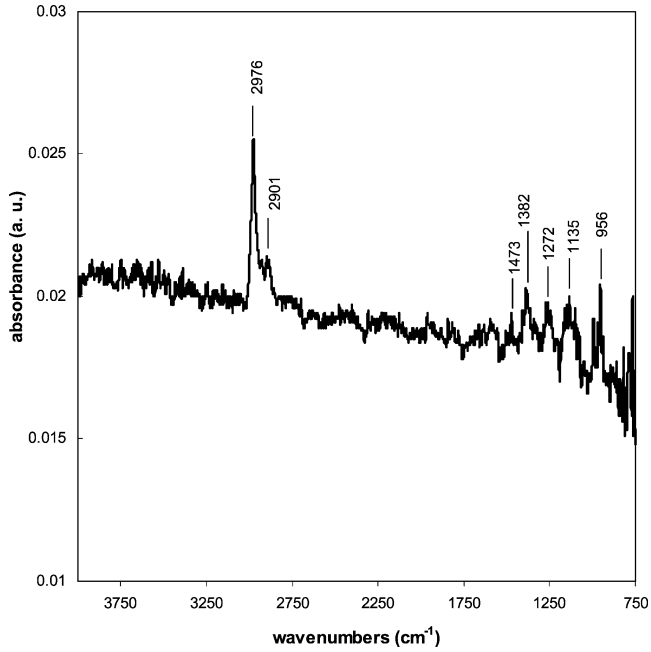

Fig. 10. DRIFT spectrum for 0.98% Cu/AC-HTT-H_2 reduced at 573 K under reaction conditions (14 Torr IPA, 448 K). Vapor-phase IPA has been subtracted from the spectrum.

tureless after the vapor-phase IPA spectrum was subtracted. As a result of IPA adsorbed onto Cu, bands are present at 2976 and 2901 cm^{-1} which are assigned to $\nu(CH_3)$ (C–H stretching vibrations), along with bands of varying intensity at 956, 1135, 1272, and 1382 cm^{-1}. After subtraction of vapor-phase IPA, the ν(OH) mode (O–H stretching vibration) at 3663 cm^{-1} cannot be detected, which indicates a very weak interaction between adsorbed IPA and the catalyst which results in little or no shift in the IR bands. The peak at 1272 can be assigned to a δ(OH) bending mode in molecularly adsorbed IPA based on the work of Zawadski et. al. [26]. The absence of a 3663 cm^{-1} band and the presence of a strong band at 2976 cm^{-1} along with the bands 956, 1135, 1382, and 2901 cm^{-1} indicate an adsorbed isopropoxide species on the surface [26–28]. Prominent bands at 1710, 1369, 1220, and 1101 cm^{-1} have been reported for acetone adsorbed on Cu/carbon films [26]; consequently, this spectrum provides no evidence for acetone adsorbed on the surface, which is most likely related to the low conversions of IPA in the DRIFTS cell because no vapor phase acetone was detected by IR. However, a low heat of adsorption, as indicated in Table 9, would also contribute to low coverage.

Table 8
Reaction orders for isopropyl alcohol dehydrogenation over 0.98% Cu/AC-HTT-H_2[a]

T_{RXN}	Reaction order		
	Isopropanol	H_2	Acetone
433	0	−0.11	−0.11
448	0.04	−0.07	−0.10
458	0.14	−0.05	−0.05
473	0.34	−0.04	0

[a] Reduced at 573 K.

4. Discussion

The dehydrogenation of alcohols to the corresponding aldehyde or ketone is well established in industrial practice, and the reaction can generally be described by the equation

$$R^1\text{–CHOH–}R^2 \rightarrow R^1\text{–CO–}R^2 + H_2, \quad (2)$$

where $R^2 = H$ for primary alcohols or an alkyl or aryl group for secondary alcohols. Tertiary alcohols cannot be dehydrogenated without rearrangement, and under typical conditions for dehydrogenation they usually dehydrate to an alkene and water [2]. This side reaction with primary and secondary alcohols that can even predominate in some cases if acidic sites are present. Methanol dehydrogenation

Table 9

Optimized rate parameters in Eq. (17) for 0.98% Cu/AC-HTT-H_2

Temperature (K)	k (μmol s^{-1} g cat^{-1})	K_{Ipa} (atm^{-1})	$K' \times 10^{-12}$	K_{H_2} (atm^{-1})	K_{Ace} (atm^{-1})
433	0.73	41.2	6.27	0.103	25.8
448	1.63	37.4	3.41	0.062	18.1
458	2.92	30.5	2.12	0.047	12.9
473	6.89	21.0	0.86	0.027	6.9

Kinetic and thermodynamic parameters for IPA dehydrogenation

E_{rds} (kcal	ΔH^0_{ad} (kcal mol^{-1})			ΔS^0_{ad} (cal mol^{-1} K^{-1})			S^0_g (cal mol^{-1} K^{-1})		
mol^{-1})	Ipa	H_2	Ace	Ipa	H_2	Ace	Ipa	H_2	Ace
22.9	−6.8	−13.4	−13.3	−8	−35	−24	68[a]	36[b]	71[c]

[a] Taken from Ref. [78].
[b] Taken from Ref. [84].
[c] Taken from Ref. [74].

to formaldehyde or methyl formate has been studied in some detail [29–34], and Cu, Ag, Zn, In, and Fe, as well as various bimetallic systems, are active catalysts. The catalytic dehydrogenation of ethanol to acetaldehyde represents an alternative to Wacker chemistry [35,36], but selectivity issues are critical because of competing dehydrogenation and decomposition reaction pathways, and ethanol decarbonylation is favored over dehydrogenation on some supported catalyst systems [37–39].

Isopropyl alcohol (IPA) dehydrogenation to acetone involves a secondary alcohol, whereas both R^1 and R^2 are methyl groups in Eq. (1). The competing dehydration reaction produces propylene and water, and this reaction has been studied over various metal oxides and zeolites [40–51]. Dehydration reactions are acid-catalyzed; thus Gervasini and Auroux were able to correlate the strength of acid sites of a metal oxide determined microcalometrically with the rate of dehydration [42]. IPA dehydrogenation proceeds on metals, and both Cu chromite and $Cu/ZnO/Al_2O_3$ are well-known active catalysts [52–54], while Pt, Ni, and Ru have also shown high activity for alcohol dehydrogenation [55–58]. Copper is of particular interest because it possesses high selectivity for the alcohol dehydrogenation reaction; however, catalysts with high copper content are typically required and the predominant copper catalyst for these reactions is Cu chromite [2], which can contain 30 to 50 wt% copper [16]. Such catalysts possess high selectivity and satisfactory activity but, unfortunately, their industrial use has been curtailed by recent regulations that prevent their disposal in landfills due to fears of hexavalent Cr. Carbon-supported Cu catalysts represent a potential replacement because the physical and chemical properties of carbon enable it to withstand the temperatures required for dehydrogenation reactions and make it impervious to strong basic or acidic reaction media. In addition, the surface properties of a carbon support can be tailored to alter the selectivity and activity of the catalyst, as demonstrated recently for one hydrogenation reaction [59].

The mechanism of IPA dehydrogenation on metal surfaces has not been the subject of many investigations [60,61], although Kraus and co-workers have studied the mechanistic aspects of IPA dehydrogenation and have speculated on the identification of active centers on chromia [60]. No study of this reaction over Cu/C catalysts was found in the literature. Consequently, this work was conducted to establish the catalytic behavior of IPA dehydrogenation over a family of Cu catalysts that had been thoroughly characterized, and the kinetics of IPA dehydrogenation were determined to allow the proposal of a reaction mechanism.

The characterization of a Norit carbon similar to that used in this study by TPD, XRD, and DRIFTS has been previously reported [10]. The modification of carbon materials either by heat treatment or by the addition of acidic or basic groups to the surface can have a significant impact on their surface properties and on the dispersion of a metal such as Cu [17]. However, in the Cu/C catalysts studied here, Cu dispersions based on chemisorption methods were routinely low (0.02–0.17) and provided estimated average crystallite sizes between 6 and 60 nm, as shown in Table 5. Crystallite sizes from XRD line broadening fell between 8 and 16 nm. With the exception of the 5.01% $Cu/AC\text{-}HTT\text{-}H_2$ sample pretreated only in He and the 4.96% $Cu/AC\text{-}HNO_3$ sample reduced at 423 K, metallic copper surface atoms, Cu_s^0, dominated. It is possible that additional reduction to Cu_s^0 could occur under reaction conditions as H_2 was generated, and this might account for the initial time-dependent activity increases shown in Fig. 4.

All carbon samples possessed some initial decomposition activity that deteriorated with time on stream to zero after 1–6 h on stream, except for $AC\text{–}HNO_3$, which maintained dehydration activity for over 20 h at which time it apparently reached a steady-state value. The dehydration of alcohols is known to occur through an E1 mechanism (elimination via a carbocation intermediate) which is catalyzed by acidic sites [62]. This carbon initially had a low dehydrogenation activity which disappeared after 3 h on stream.

TPD spectra with $AC\text{-}HNO_3$ carbon samples have shown that as the temperature increases, there is an increase in the amounts of CO_2 and CO desorbed, with CO_2 desorption corresponding to the loss of surface acidic groups [10]. Higher pretreatment temperatures result in greater acidic site loss and, as shown in Table 6, an $AC\text{-}HNO_3$ sample pretreated at 573 K has a lower dehydration rate than a sample reduced at 423 K. Moreno-Castilla et al. studied methanol dehydration to dimethyl ether over oxidized activated carbon with varying surface acidic character and found that carbons treated with $(NH_4)_2S_2O_8$ had the strongest acid groups and were the most active for dehydration [63]. The work of Szymański and Rychlicki also demonstrated that carboxyl groups were the carbon surface functionalities responsible for the dehydration of *n*-butanol to *cis*- and *trans*-butene [64]. Similar sites are associated with the dehydration activity of $AC\text{-}HNO_3$ in this study.

The dehydrogenation activity of these Cu/C catalysts, as well as the initial distribution of Cu oxidation states, was dependent upon both the catalyst pretreatment and the initial chemical state of the carbon surface, as indicated by Table 7. Fig. 4 demonstrates that a catalyst pretreated in He for 1 h at 473 K had low initial dehydrogenation activity followed by an induction period in which the generation of H_2 via IPA dehydrogenation must reduce the precursor Cu oxides to Cu^0. Cunningham et al. have shown, using high purity Cu^0, CuO, and Cu_2O powders, that the activity for IPA dehydrogenation is dependent upon the Cu oxidation state, and Cu_2O and CuO display dehydrogenation activity only after a significant induction period which is dependent on the extent of prior reduction [65]. The initial rate of dehydrogenation (after 30 min on stream) over 5.01% $Cu/AC\text{-}HTT\text{-}H_2$ treated in He at 473 K was 0.9 $\mu mol\, g^{-1}\, s^{-1}$, while the initial activities of the samples reduced at 473 and 573 K were 3 and 1.8 $\mu mol\, g^{-1}\, s^{-1}$, respectively. Cu_s^{1+} sites initially predominated in the He-treated sample, whereas the sample reduced at 473 K contained both cuprous and metallic Cu

sites and that reduced at 573 K had almost all Cu_s^0. It is possible that a synergism between Cu^0 and Cu^{1+} oxidation states may exist during IPA dehydrogenation, which is consistent with behavior reported for IPA dehydrogenation on Cu powders [65] and also for crotonaldehyde hydrogenation on Cu [59]. Dandekar et al. have shown that the turnover frequency (TOF) in the latter reaction, based on surface Cu atoms, is dependent upon the ratio of Cu_s^0/Cu_s^{1+} surface sites, with a value near unity found to be optimal [59]. However, if the above initial rate data are normalized to TOFs by the appropriate Cu_s^0 and/or Cu_s^{1+} concentrations, the relative order is $Cu_s^{1+} + Cu_s^0$ ($2.6 \times 10^{-2}\,s^{-1}$) > Cu_s^{1+} ($1.7 \times 10^{-2}\,s^{-1}$) > Cu_s^0 ($1.4 \times 10^{-2}\,s^{-1}$); thus only a small synergistic effect, if any, exists, and Cu^0 is presumed to constitute the principal catalytic site. The steady-state TOF values listed in Table 7 for 5.01% Cu/AC-HTT-H_2 after these three pretreatments assume no change in dispersion, and the relative values remain consistent. Fridman and Davydov have reported that the oxidation state of Cu can affect not only the dehydrogenation activity but also the selectivity, and in their study of cyclohexanol dehydrogenation over Cu–Mg and Cu–Zn–Al catalysts, they found that Cu^{1+} was significantly more active than Cu^0 for cyclohexanone formation, while Cu^0 was active for the aromatization reaction of cyclohexanol to phenol [66]. Chong et al. have demonstrated that the oxidation state of a $UO_2(111)$ single crystal is critical in determining the selectivity of ethanol dehydrogenation to acetaldehyde because U suboxide sites were twice as active for ethanol dehydration as for dehydrogenation [67].

There is significant evidence in the surface science literature that an alkoxide species is formed during the decomposition of various alcohols on single crystals [23,68–71] and, in fact, Xu and Friend have shown that this alkoxide (isopropoxide, in this case) is a very stable intermediate and does not dehydrogenate further to acetone until ∼270 K [71]. Behavior on single crystals suggests that the removal of the α-hydrogen from a surface isopropoxide species is the rate-determining step at low temperatures; unfortunately, no thorough kinetic studies of alcohol dehydrogenation have been conducted on supported metal catalysts.

Dehydrogenation activity is defined by the rate of formation of acetone, which is the only product observed over 0.98% Cu/AC-HTT-H_2; therefore, the overall rate of isopropanol disappearance, r_{Ipa}, is equal to the rate of acetone formation, r_{Ace}. Blank runs with pure AC-HTT-H_2 have shown that it is inert for both dehydrogenation and dehydration; thus a two-site model in which acetone is formed on copper and IPA dehydrates to propylene on acidic sites located on the carbon surface is not required. Modeling efforts with the 4.96% Cu/AC-HNO_3 catalyst would require the use of a two-site model where dehydrogenation and dehydration occur on separate and distinct surface sites.

From the partial pressure dependencies on IPA, H_2, and acetone, based on the results in Figs. 7–9, some observations pertinent to the derivation of a mechanism should be noted. For 0.98% Cu/AC-HTT-H_2, the reaction order in IPA increases with increasing temperature, which is consistent with a lower fractional surface coverage of IPA, θ_{Ipa}, with increasing temperature, as expected from a Langmuir isotherm. At all temperatures the reaction order in H_2 is zero or slightly negative, suggesting that competitive adsorption between IPA and H_2 is occurring, and the H_2 reaction order tends toward zero with increasing temperature, which indicates that H_2 adsorption also decreases with increasing temperature. The effect of acetone partial pressure on kinetic behavior also indicates product inhibition via competitive adsorption which decreases with increasing temperature. Heat of adsorption values for IPA and acetone on a clean Pt(111) are relatively low (ca. 10 kcal mol^{-1}) and indicate that an alcohol and its corresponding ketone have approximately equal affinities for adsorption on a Pt surface [72, 73]. Similar low values might be expected for copper.

Based on these observations and the application of surface science studies to C-supported Cu catalysts, a number of reaction mechanisms assuming Langmuir–Hinshelwood kinetics were proposed and examined [11]. IPA adsorption was considered to occur molecularly, and quasi-equilibrium between vapor-phase and adsorbed IPA was assumed. The formation of a hydrogen molecule from IPA was assumed to occur in two sequential elementary steps on the catalyst surface, two mechanisms were considered based on a typical Langmuir–Hinshelwood approach, and the rate expression derived from each model was tested. In one case, removal of the first hydrogen is assumed to be the rate-determining step (rds) and the abstraction of the second hydrogen is quasi-equilibrated, whereas in the other model, the removal of the first hydrogen is quasi-equilibrated and abstraction of the second hydrogen is the rds. In either case, the first hydrogen atom removed is most likely the hydroxyl hydrogen because of the previous observations of surface isopropoxide species [23,68–71]. Even though the O–H bond is probably several kcal mol^{-1} stronger than the C–H bonds in IPA [62,74], its cleavage prior to the C–H bond is probably due to its orientation on the surface. The second hydrogen atom refers to α-hydrogen, i.e., the H atom attached to the hydroxyl carbon. Although this C–H bond appears to be somewhat weaker in isopropanol than the hydroxyl bond, the catalytic pathway apparently favors the rupture of the stronger band first in a rate-determining step to give a relatively stable isopropoxide intermediate [69]. Recombinative desorption of H atoms and acetone desorption are assumed to be quasi-equilibrated.

The reaction sequence for the former model is depicted in the following equations, which represent elementary steps in which $*$ is an active site:

$$(CH_3)_2CHOH + * \overset{K_{Ipa}}{\rightleftharpoons} (CH_3)_2CHOH^*, \tag{3}$$

$$(CH_3)_2CHOH^* + * \overset{k_1}{\rightarrow} (CH_3)_2CHO^* + H^*, \tag{4}$$

$$(CH_3)_2CHO^* + * \overset{K_2}{\rightleftharpoons} (CH_3)_2CO^* + H^*, \tag{5}$$

$$(CH_3)_2CO^* \overset{1/K_A}{\rightleftharpoons} (CH_3)_2CO + {}^*, \tag{6}$$

$$2H^* \overset{1/K_{H_2}}{\rightleftharpoons} H_2 + 2^*. \tag{7}$$

If removal of the first hydrogen atom (hydroxyl hydrogen) is assumed to be an irreversible rds, the formation of acetone, r_{Ace}, is

$$r_{Ace} = Lk_1\theta_{Ipa}\theta_v, \tag{8}$$

where L is the total number of active sites, k_1 is the forward rate constant of reaction (4); θ_{Ipa} is the fractional coverage of isopropanol, and θ_v is the fraction of vacant sites. The respective expressions for quasi-equilibrated adsorption of isopropyl alcohol, hydrogen, and acetone on the Cu surface are

$$K_{Ipa} = \frac{\theta_{Ipa}}{P_{Ipa}\theta_v}, \tag{9}$$

$$K_{H_2} = \frac{\theta_H^2}{P_{H_2}\theta_v^2}, \tag{10}$$

$$K_{Ace} = \frac{\theta_{Ace}}{P_{Ace}\theta_v}. \tag{11}$$

This reaction order study has shown that H_2 and acetone have a small inhibitory effect when added to the feed stream, and this leads to the inclusion of both hydrogen and acetone species in the site balance along with a molecularly adsorbed isopropanol species. The presence of IPA and an isopropoxide species in the site balance was justified by the in situ DRIFT spectrum obtained during IPA dehydrogenation. The coverage of the isopropoxide species, θ_{Iso}, is governed by steps (5)–(7) and is represented by:

$$\theta_{Iso} = K_{Ace}K_{H_2}^{1/2}K_2^{-1}P_{Ace}P_{H_2}^{1/2}\theta_v. \tag{12}$$

The inclusion of all four species in the site balance, i.e.,

$$1 = \theta_{Ipa} + \theta_H + \theta_{Ace} + \theta_{Iso} + \theta_v, \tag{13}$$

and utilization of Eqs. (9)–(12) gives

$$1 = K_{Ipa}P_{Ipa}\theta_v + K_{H_2}^{1/2}P_{H_2}^{1/2}\theta_v + K_{Ace}P_{Ace}\theta_v + \frac{K_{Ace}K_{H_2}^{1/2}}{K_2}P_{Ace}P_{H_2}^{1/2}\theta_v + \theta_v, \tag{14}$$

which yields

$$\theta_v = \left(1 + K_{Ipa}P_{Ipa} + K_{H_2}^{1/2}P_{H_2}^{1/2} + K_{Ace}P_{Ace} + \frac{K_{Ace}K_{H_2}^{1/2}}{K_2}P_{Ace}P_{H_2}^{1/2}\right)^{-1}. \tag{15}$$

Substitution of θ_{Ipa} from Eq. (9) into Eq. (8) yields

$$r_{Ace} = Lk_1K_{Ipa}P_{Ipa}\theta_v^2 \tag{16}$$

and the final rate expression is

$$r_{Ace} = kK_{Ipa}P_{Ipa}\left(1 + K_{Ipa}P_{Ipa} + K_{H_2}^{1/2}P_{H_2}^{1/2} + K_{Ace}P_{Ace} + K'P_{Ace}P_{H_2}^{1/2}\right)^{-2}, \tag{17}$$

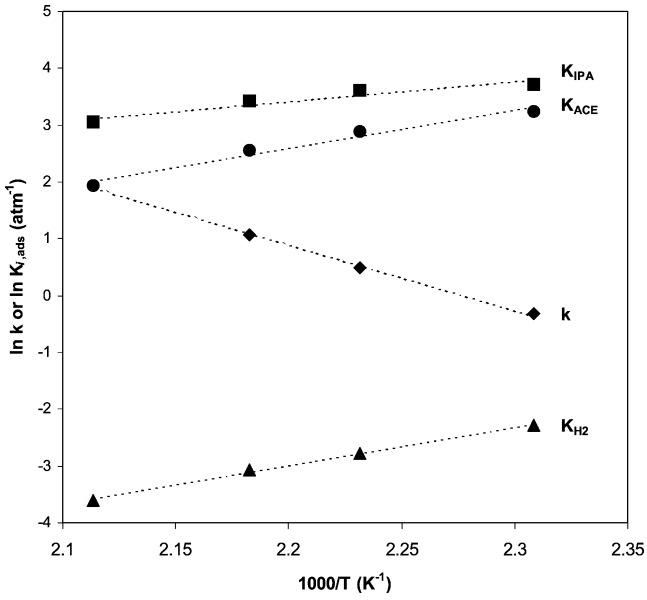

Fig. 11. Rate constant, k, and equilibrium adsorption constants, K_i, from Table 9 versus inverse temperature.

where $k = Lk_1$ and $K' = K_{Ace}K_{H_2}^{1/2}/K_2$.

Eq. (17) was fitted to the experimental results using Scientist, a commercially available data-fitting program which uses a least-squares nonlinear optimization method utilizing a modified Powell algorithm to find the minimum of the sum of squared deviations between observed and model calculations [75]. To ensure that a global minimum had been obtained, an iterative process was initiated which used a number of different initial guesses for each value. The optimized parameters for the four constants at four temperatures are listed in Table 9, and the fits to the experimental data are shown in Figs. 7–9. Values listed for the rate constant k in Table 9 essentially represent the rate constant k_1 for the rds, and it increases with temperature. Consistent with thermodynamic expectations, equilibrium adsorption constants (K_i) decrease with increasing temperature and a plot of $\ln K_i$ versus $1/T$ will yield values for $\Delta S^0_{ad,i}$, the standard entropy of adsorption, and $\Delta H^0_{ad,i}$, the standard enthalpy of adsorption. These plots are shown in Fig. 11, and these thermodynamic values for IPA, H_2, and acetone are also listed in Table 9.

Insight into the validity of the proposed reaction model can be obtained by subjecting the ΔS^0_{ad} values to two strong rules: (1) ΔS^0_{ad} must be negative and (2) ΔS^0_{ad} must have an absolute value smaller than S^0_g, the standard entropy in the vapor phase [76,77]. If rule 1 or 2 is violated, then the values of K have no physical meaning in the Langmuirian sense. A third, less stringent guideline indicates that the minimum value of ΔS^0_{ad} is approximately -10 entropy units (1 e.u. = cal mol^{-1} K^{-1}), which represents a loss of approximately one degree of translational freedom [76,77]. Concurrently, the enthalpy of adsorption must be negative, as adsorption is always exothermic and the true rate constant must display proper Arrhenius behavior. The enthalpy of ad-

sorption for IPA on Cu is lower than that for IPA on Pt (10.6 kcal mol^{-1}) [72], and this indicates that IPA is weakly adsorbed and should be quite mobile on the surface, consistent with the $\Delta S^0_{\mathrm{ad,IPA}}$ value. The absolute entropy of IPA in the vapor phase at a temperature representative of experimental conditions is 68 e.u. [78]. In the case of hydrogen adsorption, the enthalpy of adsorption indicates a stronger affinity between Cu and H, compared to IPA, and the $\Delta H^0_{\mathrm{ad,H_2}}$ value of -13.4 kcal mol^{-1} is in agreement with integral heat of adsorption values for H_2 on Cu [79,80], but significantly lower than values measured on Cu single crystals in the low coverage regime [81–83]. The ΔS^0_{ad} value of -35 e.u. for H_2, which is close to the S^0_{g} value of 36 e.u. [84], suggests that the catalytically active H atoms are immobile on the Cu surface. The absolute entropy for acetone is similar to that for IPA, and the adsorption parameters for acetone imply stronger bonding on the Cu surface than with IPA, and the ΔH_{ad} value is near that found for acetone on Pt(111), i.e., 12 kcal mol^{-1} [73]. The inhibitive effect of acetone is low due to the high partial pressures of isopropanol and low conversions, so acetone partial pressures are low. This explanation is consistent with the in situ DRIFTS spectrum under reaction conditions because a carbonyl stretch band near 1710 cm^{-1} for acetone was not observed. Similar fits are obtained if the surface isopropoxide species is omitted from the site balance depicted by Eq. (13), and the only significant effect on the thermodynamic parameters is a decrease in the ΔH_{ad} and ΔS_{ad} values for acetone such that they become similar to those for IPA [11]. Also, if removal of the second H atom is assumed to be the rds (model 2), a negative dependence of $-1/2$ or greater exists for H_2, which is inconsistent with the results in Table 8; thus this model was discarded [11].

Because of its selectivity benefits, Cu is the metal of choice in such dehydrogenation reactions even though it has a lower specific activity than noble metals. The reasons for this are not well established, and this aspect of selectivity vs activity in these reactions would seem worthy of investigation, especially in view of the impact that GpVIII/Gp Ib bimetallic systems and SMSI catalysts have had on hydrogenation reactions.

In more complicated reactions, such as liquid-phase citral hydrogenation, which produces numerous intermediates, the use of kinetic data obtained in a semibatch reactor free from heat and mass transfer artifacts to describe a network of parallel and sequential catalytic reactions has been demonstrated, and a deactivating side reaction was also incorporated into this reaction model [3]. Again, a thermodynamic analysis of the rate parameters demonstrated the consistency of the model proposed.

5. Summary

Isopropyl alcohol dehydrogenation over carbon-supported Cu catalysts was studied and compared to UHP Cu powder and a Cu chromite catalyst. Low dispersions of Cu (ca. 0.02–0.17) were obtained in all these supported catalysts. The measurement of surface Cu atom concentrations allowed turnover frequencies to be calculated so that an accurate comparison of specific activity could be made. Cu dispersed on a high-temperature-treated (HTT) activated carbon had the highest turnover frequency of all the Cu/C catalysts, and it was comparable to or higher than that of an industrial Cu chromite catalyst. The steady-state selectivity to acetone was 100% for all catalysts except those containing the nitric acid treated carbon. In the absence of Cu, the nitric-acid-treated carbon retained a steady-state activity for propylene formation, but reduction at 573 rather than 423 K decreased this activity. This dehydration reaction was associated with the presence of oxygen-containing acidic groups on the C surface. The apparent activation energy for acetone formation was typically near 20 kcal mol^{-1} for all the Cu/C catalysts and the Cu powder, but it was near 12 kcal mol^{-1} for the Cu chromite catalyst. A DRIFT spectrum under reaction conditions indicated the presence of an isopropoxide species and molecularly adsorbed IPA on the surface. A Langmuir–Hinshelwood mechanism, which assumed removal of the first hydrogen atom as the rate-determining step and incorporated adsorbed IPA, hydrogen, acetone, and a surface isopropoxide species into the site balance, fit the kinetic data well. Analysis of the parameters in the rate expression using thermodynamic guidelines showed that they contained physically meaningful values for the enthalpies and entropies of adsorption.

Acknowledgment

This study was financially supported by the NSF via Grant CTS-9903559.

References

[1] (a) F. Buonomo, D. Sanfilippo, F. Trifiro, in: G. Ertl, H. Knözinger, J. Weitkamp (Eds.), Handbook of Heterogeneous Catalysis, Vol. 5, Wiley–VCH, Weinheim, 1997, p. 2140;
(b) K. Kochloefl, in: G. Ertl, H. Knözinger, J. Weitkamp (Eds.), Handbook of Heterogeneous Catalysis, Vol. 5, Wiley–VCH, Weinheim, 1997, p. 2151.
[2] M. Kraus, in: G. Ertl, H. Knözinger, J. Weitkamp (Eds.), Handbook of Heterogeneous Catalysis, Vol. 4, Wiley–VCH, Weinheim, 1997, p. 2159.
[3] U.K. Singh, M.A. Vannice, Appl. Catal. A Gen. 213 (2001) 1.
[4] G.C. Bond, Catalysis by Metals, Academic Press, New York, 1962.
[5] P.B. Weisz, Z. Phys. Chem. 11 (1957) 1.
[6] E.W. Thiele, Ind. Eng. Chem. 31 (1939) 916.
[7] R.J. Madon, M. Boudart, Ind. Eng. Chem. Fund. 21 (1982) 438.
[8] G. Ertl, H. Knözinger, J. Weitkamp (Eds.), Environmental Catalysis, Wiley–VCH, Weinheim, 1999.
[9] J. Armor (Ed.), Environmental Catalysis, in: ACS Symposium Seriers, Vol. 552, Am. Chem. Society, Washington, DC, 1994, p. 372.
[10] A. Dandekar, R.T.K. Baker, M.A. Vannice, Carbon 36 (1998) 1821.
[11] R.M. Rioux, MS thesis, The Pennsylvania State University, 2001.
[12] D. Richard, P. Gallezot, in: B. Delmon, P. Grange, P.A. Jacobs, G. Poncelet (Eds.), Preparation of Catalysts IV, Elsevier, Amsterdam, 1987, p. 71.

[13] J.P. Brunelle, Pure Appl. Chem. 50 (1978) 1211.
[14] M.A. Kohler, J.C. Lee, D.L. Trimm, N.W. Cant, M.S. Wainwright, Appl. Catal. 31 (1987) 309.
[15] H. Kobayashi, N. Takezawa, C. Minochi, K. Takahashi, Chem. Lett. (1980) 1197.
[16] Engelhard Corporation Technical Literature, Copper Chromite Product Data Sheet, 1996.
[17] A. Dandekar, R.T.K. Baker, M.A. Vannice, J. Catal. 183 (1999) 131.
[18] A. Dandekar, M.A. Vannice, J. Catal. 178 (1998) 621.
[19] R.E. Rondeau, J. Chem. Eng. Data 10 (1965) 124.
[20] J.J. Venter, M.A. Vannice, Appl. Spectrosc. 42 (1988) 1096.
[21] P.E. Fanning, M.A. Vannice, Carbon 31 (1993) 721.
[22] C. Moreno-Castilla, O.P. Mahajan, P.L. Walker Jr., H.-J. Jung, M.A. Vannice, Carbon 18 (1980) 271.
[23] G. Djega-Mariadassou, A.R. Marques, L. Davignon, J. Chem. Soc. Faraday Trans. I 78 (1982) 2447.
[24] J.H. Sinfelt, J.L. Carter, D.J.C. Yates, J. Catal. 24 (1972) 283.
[25] B. Echevin, S.J. Teichner, Bull. Soc. Chim. Fr. 7 (1975) 1495.
[26] J. Zawadzki, M. Wiśniewski, J. Weber, O. Heintz, B. Azambre, Carbon 39 (2001) 187.
[27] J.L. Davis, M.A. Barteau, Surf. Sci. 235 (1990) 235.
[28] R.F. Rossi, G. Busca, V. Lorenzelli, O. Saur, J.C. Lavalley, Langmuir 3 (1987) 52.
[29] S. Su, P. Zaza, A. Renken, Chem. Eng. Technol. 17 (1994) 34.
[30] R. Zhang, Y.-H. Sun, S.-Y. Peng, React. Kinet. Catal. Lett. 67 (1999) 95.
[31] A. Guerrero-Ruiz, I. Rodriguez-Ramos, J.L.G. Fierro, Appl. Catal. 72 (1991) 119.
[32] E.H. Shreiber, M.D. Rhodes, G.W. Roberts, Appl. Catal. B. 23 (1999) 9.
[33] P. Zaza, H. Randall, R. Doepper, A. Renken, Catal. Today 20 (1994) 325.
[34] A. Mušič, J. Batista, J. Levec, Appl. Catal. A 165 (1997) 115.
[35] B.A. Raich, H.C. Foley, Ind. Eng. Chem. Res. 37 (1998) 3888.
[36] N. Iwasa, O. Yamamoto, R. Tamura, M. Nishikubo, N. Takezawa, Catal. Lett. 62 (1999) 179.
[37] J.M. Davidson, C.M. McGregor, L.K. Doraiswamy, Ind. Eng. Chem. Res. 40 (2001) 101.
[38] J.M. Davidson, C.M. McGregor, L.K. Doraiswamy, Ind. Eng. Chem. Res. 40 (2001) 108.
[39] H. Amandusson, L.-G. Ekedahl, H. Dannetun, J. Catal. 195 (2000) 376.
[40] T. Matsuda, H. Sakagami, N. Takahashi, Appl. Catal. A 213 (2001) 83.
[41] K. Hashimoto, N. Toukai, J. Mol. Catal. A 145 (1999) 273.
[42] A. Gervasini, A. Auroux, J. Catal. 131 (1991) 190.
[43] A. Gervasini, J. Fenyvesi, A. Auroux, Catal. Lett. 43 (1997) 219.
[44] M.A. Aramendía, V. Borau, C. Jiménez, J.M. Marinas, A. Porras, F.J. Urbano, React. Kinet. Catal. Lett. 53 (1994) 397.
[45] K.C. Waugh, M. Bowker, R.W. Petts, H.D. Vandervell, J. O'Malley, Appl. Catal. 25 (1986) 121.
[46] J.A. Wang, X. Bokhimi, O. Novaro, T. López, R. Gómez, J. Mol. Catal. A 145 (1999) 291.
[47] E. Akiba, M. Soma, T. Onishi, K. Tamaru, Z. Phys. Chem. N. F. 119 (1980) 103.
[48] F. Kooli, C. Martín, V. Rives, Langmuir 13 (1997) 2303.
[49] A. Corma, V. Fornés, F. Rey, J. Catal. 148 (1994) 205.
[50] T. Yashima, H. Suzuki, N. Hara, J. Catal. 33 (1974) 486.
[51] D. Haffad, A. Chambellan, J.C. Lavalley, J. Mol. Catal. A 168 (2001) 153.
[52] R.B.C. Pillai, Ind. J. Chem. 33 (1994) 1087.
[53] O.V. Makarova, T.M. Yur'eva, G.N. Kustova, A.V. Ziborov, L.M. Plyasova, T.P. Minyukova, L.P. Davydova, V.I. Zaikovskii, Kinet. Katal. 34 (1993) 608.
[54] O.V. Makarova, T.M. Yur'eva, L.M. Plyasova, T.A. Kriger, V.I. Zaikovskii, Kinet. Katal. 35 (1994) 471.
[55] J. Newham, R.L. Burwell Jr., J. Am. Chem. Soc. 86 (1964) 1179.
[56] Y. Ando, X. Li, E. Ito, M. Yamashita, Y. Saito, in: T. Inui, et al. (Eds.), New Aspects of Spillover Effect in Catalysis, Elsevier, Amsterdam, 1993, p. 313.
[57] S.V. Vinogradov, M.V. Ulitin, O.V. Lefedova, Russ. J. Phys. Chem. 73 (1999) 1741.
[58] D.E. Mears, M. Boudart, AIChE J. 12 (1966) 313.
[59] A. Dandekar, R.T.K. Baker, M.A. Vannice, J. Catal. 184 (1999) 421.
[60] M. Kraus, Z. Žitny, D. Mihajlova, A. Andreev, Collect. Czech. Chem. Commun. 41 (1976) 3563.
[61] L. Nondek, J. Sedláček, J. Catal. 40 (1975) 34.
[62] F.A. Carey, R.J. Sundberg, in: Advanced Organic Chemistry A, 3rd ed., Plenum, New York, 1990.
[63] C. Moreno-Castilla, F. Carrasco-Marin, C. Parejo-Perez, M. Lopez-Ramon, Carbon 39 (2001) 869.
[64] G.S. Szymański, G. Rychlicki, Carbon 29 (1991) 489.
[65] J. Cunningham, G.H. Al-Sayyed, J.A. Cronin, C. Healy, W. Hirschwald, Appl. Catal. 25 (1986) 129.
[66] V.Z. Fridman, A.A. Davydov, J. Catal. 195 (2000) 20.
[67] S.V. Chong, M.A. Barteau, H. Idriss, Catal. Today 63 (2000) 283.
[68] D.A. Chen, C.M. Friend, Langmuir 14 (1998) 1451.
[69] M.K. Weldon, C.M. Friend, Chem. Rev. 96 (1996) 1391.
[70] L.J. Shorthouse, A.J. Roberts, R. Raval, Surf. Sci. 480 (2001) 37.
[71] X. Xu, C.M. Friend, Surf. Sci. 260 (1992) 14.
[72] M.A. Vannice, W. Erley, H. Ibach, Surf. Sci. 254 (1991) 12.
[73] M.A. Vannice, W. Erley, H. Ibach, Surf. Sci. 254 (1991) 1.
[74] D.R. Lide (Ed.), CRC Handbook of Chemistry and Physics, 73rd ed., CRC Press, Boca Raton, FL, 1992.
[75] Micromath Scientific Software Manual for Scientists, Salt Lake City, 1995, p. 380.
[76] M. Boudart, D.E. Mears, M.A. Vannice, Ind. Chim. Belge 32 (1967) 281.
[77] M.A. Vannice, S.H. Hyun, B. Kalpakci, W.C. Liauh, J. Catal. 56 (1979) 358.
[78] P. Atkins, Physical Chemistry, 5th ed., Freeman, San Francisco, 1994.
[79] M. Muhler, L.P. Nielsen, E. Törnqvist, B.S. Clausen, H. Topsøe, Catal. Lett. 14 (1992) 241.
[80] T. Genger, O. Hinrichsen, M. Muhler, Catal. Lett. 59 (1999) 137.
[81] P.B. Lloyd, M. Swaminathan, J.W. Kress, B.J. Tatarchuk, Appl. Surf. Sci. 119 (1997) 267.
[82] J.T. Campbell, C.T. Campbell, Surf. Sci. 259 (1991) 1.
[83] C.T. Rettner, H.A. Michelsen, D.J. Auerbach, Faraday Discuss. 96 (1993) 17.
[84] J.D. Cox, D.D. Wagman, V.A. Medvedev (Eds.), Codata Key Values for Thermodynamics, Hemisphere Publishing Inc., 1989.